Atmos. Meas. Tech. Discuss., https://doi.org/10.5194/amt-2017-254
Manuscript under review for journal Atmos. Meas. Tech.
Discussion started: 22 August 2017

Atmospheric Measurement Techniques Discussions

A simple insect removal algorithm for 35-GHz cloud radar measurements

Madhu Chandra R. Kalapureddy[1*], Sukanya Patra[1], Subrata K Das[1], Sachin M Deshpande[1], Kaustav Chakravarty[1], Ambuj K Jha[1], Prasad Kalekar[1], Hari Krishna Devisetty[1], Andrew L Pazamany[2] and Pandithurai Govindan[1]

[1]Indian Institute of Tropical Meteorology (IITM), Dr Homi Bhabha road, Pashan, Pune 411008, Maharastra, India.
[2]Prosesning Inc., 107 Sunderland road, Amherst, MA 01002, US.

Correspondence to: Madhu Chandra R. Kalapureddy (kalapureddy1@gmail.com)

Abstract. One of the key parameters that must be included in the analysis of atmospheric constituents (gases and particles) and clouds is the vertical structure of the atmosphere. Therefore high-resolution vertical profile observations of the atmospheric targets are required for both theoretical and practical evaluation and as inputs to increase accuracy of atmospheric models. Cloud radar reflectivity profiles can be an important measurement for the investigation of cloud vertical structure in a resourceful way. However, extracting intended meteorological cloud content from the overall measurement often demands an effective technique or algorithm that can reduce error and observational uncertainties in the recorded data. In this work a technique is proposed to identify and separate cloud and non-hydrometeor returns from a cloud radar measurements. Firstly the observed cloud reflectivity profile must be evaluated against the theoretical radar sensitivity curves. This step helps to determine the range of receiver noise floor above which it can be identified as signal or an atmospheric echo. However it should be noted that the signal above the noise floor may be contaminated by the air-borne non-meteorological targets such as insects, birds, or airplanes. The second step in this analysis statistically reviews the continual radar echoes to determine the signal de-correlation period. Cloud echoes are observed to be temporally more coherent, homogenous and have a longer de-correlation period than insects and noise. This step critically helps in separating the clouds from insects and noise which show shorter de-correlation periods. The above two steps ensure the identification and removal of non-hydrometeor contributions from the cloud radar reflectivity profile which can then be used for inferring unbiased vertical cloud structure. However these two steps are insufficient for recovering the weakly echoing cloud boundaries associated with the sharp reduction in cloud droplet size and concentrations. In the final step in order to obtain intact cloud height information, identified cloud echo peak(s) needs to be backtracked along the either sides on the reflectivity profile till its value falls close to the mean noise floor. The proposed algorithm potentially identify cloud height solely through the characterization of high resolution cloud radar reflectivity measurements with the theoretical echo sensitivity curves and observed echo statistics for the cloud tracking (TEST). This technique is found to be more robust in identifying and filtering out the contributions due to insects and noise which may

Atmos. Meas. Tech. Discuss., https://doi.org/10.5194/amt-2017-254
Manuscript under review for journal Atmos. Meas. Tech.
Discussion started: 22 August 2017

Atmospheric Measurement Techniques Discussions

contaminate a cloud reflectivity profile. With this algorithm it is possible to improve monsoon tropical cloud characterization using cloud radar.

1.0 Introduction

Cloud vertical structure (CVS) associated with the monsoon cloud systems is a key parameter needs to be understood specifically in the light of its contrasting seasonal features. This allows in unraveling the role of CVS for better characterization of various types of tropical monsoon cloud systems viz., deep, shallow convective clouds and stratiform cloud systems. The high-resolution vertical profiling measurements of cloud radar are useful resource in understanding of clouds and its evolution. Furthermore this technique will aid in the statistical characterization of CVS associated with the Indian Summer Monsoon (ISM) and its intra-seasonal variability. The cloud radar system uses short millimeter-wavelengths of 3.1 and 8.5 mm which correspond to frequency is ~94 and ~35 GHz respectively. These wavelengths allow the detection of small cloud droplets and ice particles more sensibly at high spatial and temporal resolutions that is used to infer important information on microphysical and dynamical structure of cloud (e.g., Lhermitte, 1987; Frisch et al., 1995; Kollias and Albrecht, 2000; Sassen et al., 1999; Hogan et al., 2005). Cloud radar, especially 35 GHz, is not only sensitive to hydrometeors (cloud particles and rain drops) but also to air-borne biological targets such as birds and insects, and waste plant materials e.g., dry leaves, pollen or dust (also known as “atmospheric plankton” or atmospheric “biota” or simply “insects”; Lhermitte, 1966; Teschke et al., 2006). Although insects are probably the principal contaminants because of their size and dielectric constant, spiders, spider webs, and other organic materials have been detected in the atmosphere through the use of nets and other means (Sekelsky et al., 1998). Furthermore due to reduced scattering efficiency in the Mie region, cloud radar observations at 95 GHz are found to be less sensitive to insects than observations at 35 GHz (Khandwalla et al., 2003). Cloud radar signals frequently encounter this biota, within a couple of kilometers altitude close to the Earth surface, confined mostly to the Atmospheric Boundary Layer (ABL). These echoes from the insect in the ABL have reflectivity values comparable to those from the clouds and precipitation, and thus they contaminate and mask the true cloud returns (Luke et al., 2008). The identification and removal of returns from such non-meteorological targets (biota and receiver noise) is one of the prime tasks that is required to perform before using the meteorological (cloud and precipitation) returns received by the cloud radar data, for the research and analysis purpose. The current work focuses on identifying and filtering non-hydrometeor echoes in order to significantly improve the quality of cloud radar data. This allows for the improved characterization of the tropical CVS.

Review of previous studies shows that different techniques have been attempted to remove non meteorological echoes, for example, static techniques for the ground clutter (Harrison et al., 2014; 2000), return signal-level correction (Doviak and Zrni´c, 1984; Torres and Zrni´c, 1999; Nguyen et al., 2008), dynamic filtering (Steiner and Smith, 2002), and operational filtering (Alberoni et al., 2003; Meischner et al., 1997). The

Atmos. Meas. Tech. Discuss., https://doi.org/10.5194/amt-2017-254
Manuscript under review for journal Atmos. Meas. Tech.
Discussion started: 22 August 2017

Atmospheric Measurement Techniques Discussions

aforementioned studies were mostly confined with the use of single polarization radar. However a new possibility has been developed using dual-polarization information to identify the non-meteorological clutter echoes (Zrnic´ and Ryzhkov, 1998; Mueller, 1983; Zhang et al., 2005). With the advent in Doppler spectral processing, it is possible to have improved clutter mask (Bauer-Pfundstein and Görsdorf, 2007; Luke et al., 2008; Warde and Torres, 2009; Unal, 2009). As mentioned one of the non-meteorological echoes is due to the insects and air-borne biota and these unwanted echoes are problematic for studies involving meteorological information such as wind measurements (Muller and Larkin, 1985) and true cloud returns (Martner and Moran, 2001). As a consequence, observations of insects were done using variable polarization and multiple frequency radars operating initially in the centimeter wavelength (Hajovsky et al., 1966; Hardy et al., 1966; Mueller and Larkin, 1985). At millimeter wavelength radar, Bauer-Pfundstein and Görsdorf (2007) showed effective LDR filtering of insects while Khandwalla et al. (2003) and Luke et al. (2008) showed that dual-wavelength ratio filters are more effective than the linear depolarization ratio filters. Dual-polarization also offers a wide variety of methods (e.g., Gourley et al., 2007; Hurtado and Nehorai, 2008; Unal, 2009; Chandrasekar et al., 2013). Fuzzy logic classification techniques for the identification and removal of spurious echoes from radar are also in use (e.g., Cho et al., 2006; Dufton and Collier, 2015). From the above summary, it is therefore evident that most of the studies either concentrate on the polarimetric capabilities of radar or off-line spectral processing of radar data to filter out echoes contaminated by non-meteorological targets. The importance of the current work presented here lies in the development of an algorithm that uses solely high spatial and temporal resolution reflectivity measurements. These high spatial and temporal resolution (25 m and 1 sec) measurements enable the characterization of irregular echoes associated with the spurious nature of radar returns due to insects. This method is simple and does not require spacious complex spectral data (and associated complicated analysis) or expensive advanced dual-polarimetric or dual-wavelength techniques.

2.0 System, Data and Methodology

This investigation employs vertically oriented observations of IITM's Ka-band scanning polarimetric radar (KaSPR) for the study of vertical cloud structure. KaSPR has been providing high resolution (25 m and 1 sec.) resourceful measurements of cloud and precipitation at a tropical site (Mandhardev, 18.0429^0 N, 73.8689^0 E, 1.35 km AMSL) on a mobile platform since June, 2013. Its main technical features are given in Table 1. KaSPR possess sensitivity of above -60 (-45) dBZ at 1(5) km, it is therefore sensitive to the cloud droplet. According to T-matrix computations, single 0.1 mm size of target at ~35 GHz may have the reflectivity ~ -60 dBZ whereas near one million (63) of 0.01 (0.05) mm size is required to give the same reflectivity. Furthermore in one second if there are 500 (pulses per second) hits on the target in the radar scattering volume, the mean of those 500 samples at a range bin (height) will be affected by the mean characteristics of target such as composition, orientation, number density and kinematics associated with it. Therefore it is safer to assume that the atmospheric or meteorological targets (in this case cloud particle) are distributive in nature and passive in the sense that their motion and/or orientation are in resonance with the kinematics of the background atmosphere. By comparison birds and insects are point targets in nature and active in the sense that they can change their motion, direction and orientation within a few seconds. This

leads to the irregular nature of intermittent or spurious radar returns characteristic of atmospheric biota due to the much smaller de-correlation time associated with them. This study utilizes the high resolution profile of cloud radar reflectivity factor (Z) to construct the cloud vertical structures by filtering out the returns from the noise and insects.

Figure 1a represents the height profiles of Z on 27 Apr 2014 at 2303 UT with various theoretical radar sensitivity (noise-equivalent reflectivity, NER) curves (S0-S5; the range profile correction with the start range sensitivity value of reflectivity, i.e., $r^2xZ_{start\ range}$, where r is range or height and Z is reflectivity, for S1, Z is -60 dBZ, for example). These different NER or sensitivity curves are utilized to qualify the observed radar returns that are indeed above the NER, the inherent radar receiver noise level. The receiver noise level is the inherent thermal noise associated with electronic components in the receiver chain and it remains approximately constant over the length of the pulse returns. However, range correction is intuitive in the radar equation due to the decrease in echo signal strength with increasing height (for vertical orientation). In order to determine the noise range in every range bin, S0 to S5 are computed and overlaid on Z. This allows for identification and characterization of the signal that overlays the background system noise level. As discussed earlier, the signal at any level may have contributions due to either volumetric meteorological cloud particulates and/or strong non-meteorological point targets (e.g. biota). In Figure 1a the echoes at ~3.7 km and below 2 km can be marked as cloud and insects respectively as it exceeds the profile S5. The noise variations around 15 dB are mostly confined in between S0 and S2 with S1 as mean NER. Contrasting echo texture associated with the cloud and atmospheric biota (hereafter insect) is evident from the height-time-intensity (HTI) plot of Z in Figure 1b. This is a weak cloud case having reflectivity ~ -38 dBZ at ~3.7 km altitude with the presence of intermittent, non homogeneous echo texture from the insects below 2.7 km altitude. Near similar weak cloud case of -38±2 dBZ at 5.4 km altitude is confirmed as cloud with the sharp increase in relative humidity of ~ 80% at that altitude by collocated GPS-RS measurements but is not shown here. Insect echoes are observed to be confined most densely below 1.7 km and fall in the reflectivity range of -50 to -20 dBZ. The observed standard deviation is always more than 2 and de-correlation period of ~4-5 sec (returns due to insects is found to vanish at an interval of ~3-8 sec). Two sensitivity (S1 and S5) tests have been performed on Z profile to quantify as the meteorological cloud returns. All the tests have been affected due to the presence of non-meteorological echo due to insects even though these are mostly present in the ABL. Reflectivity values associated with the cloud boundaries are very faint and are noticed to be fall within or close to system noise floor by 2-5 dB. The profile S5 seems to be better in screening out the cloud echoes by 10 dBZ higher level than system mean noise floor but this can eliminate significant portion of the weakest reflectivity area at the cloud edge (Figure 1d). Apart from clouds, insects also show higher reflectivity values than S5. Figure 1d is similar to Figure-1b except, it is completely screened out for cloud by applying typical threshold of radar system sensitivity profile, S1 and S5. In addition to this, in case of Figure 1c, contiguous set of four reflectivity profiles have been considered for computing running mean and standard deviation. The method followed to generate Figure 1c is the main objective of this paper and is outlined by the flowchart in Figure 6. This method will be fully explained in the following section. In this case, insect reflectivity values are similar to those of the cloud but their altitude levels are significantly different. The contribution due to insects can therefore be removed by fixing with S5 and leaving the contribution due to

Atmos. Meas. Tech. Discuss., https://doi.org/10.5194/amt-2017-254
Manuscript under review for journal Atmos. Meas. Tech.
Discussion started: 22 August 2017

clouds untouched (Figure 1d). Thus, for the simultaneous presence of cloud and insect echoes at around same altitude this NER method fails to identify the contributions separately. This NER method also fails whenever there exist sharp reflectivity changes, usually seen with cloud boundaries/edges. This issue therefore demands the development of a robust algorithm that explores the fundamental difference between cloud and insect returns so that it could be identified and separated out these factors automatically.

In order to make the algorithm more robust for running it automatically, a close re-inspection of Figure 1b infers that cloud returns are much more regular and near homogeneous when compared to insect's returns, which appears to be spurious or intermittent in occurrence. Therefore, the NER criterion works reasonably well for the case of homogeneous, isolated stable cloud layers but its robustness will be in question whenever there are vigorous and quick changes associated with cloud edge and/or structure (will be explained in the discussion of cloud 1-2 in Figure 5). An additional criterion makes the current algorithm robust for complete revival of cloud information from the Z observations by utilizing the de-correlation periods of insects (close to 3-5 sec). During this time interval significant changes are not seen within the cloud. To explore this fact, in the next section the same weak low level cloud case has been chosen further to understand the coherence period associated with cloud and insects.

3.0 Results and Discussions

Figure 2 takes the same case as in Figure 1 but confined below 4 km and 80-300 s, (left panel). Figure 2 reveals three main type of radar echo region namely (1) consistent radar returns characterized by the smooth and gradual change(s) associated with cloud particles (at ~ 3.7 km height), (2) sharp (gradient) and spurious radar returns (at altitude below 2.7 km) due to point target(s) and (3) receiver noise floor. In order to locate the above echo types easily, various sensitivity or NER (i.e., S0-S5) curves have been utilized. The second type of echo is associated with a characteristic point target (which has sharp reflectivity gradient feature due to the target's limited spatial as well as temporal spread associated with the radar scattering volume). The third type, noise floor, is seen to be confined mostly in between S0 and S2. The right panel in Figure 2 corresponds to HTI plot where the echo texture pertinent to the above mentioned three echo types can be clearly visualized. The cloud echoes spreads in the altitude region of approximately 300 m (3.6-3.9 km) with consistent smooth and gradual evolution with its weakest and/or broken structure during 165-190s. In contrast to this the observed irregular point or rounded texture of insects echo spread is seen to be limited temporally around 3-7 seconds and spatially below four range-bins size (i.e., < 100 m) with strongest reflectivity at its center. This indicates that one second temporal resolution might be good enough to see the insects as point or rounded echo texture. When biota density is more in the lower altitude levels, it is difficult to clearly identify the boundary of one point target from another. Such a scenario, though rare, can lead to misidentification as clouds. The coexistence of cloud and transient high density flocks of biota adds complexity which becomes almost impossible to discriminate. However, this issue is observed to be rare and limited to lowest altitudes only.

Atmos. Meas. Tech. Discuss., https://doi.org/10.5194/amt-2017-254
Manuscript under review for journal Atmos. Meas. Tech.
Discussion started: 22 August 2017

Atmospheric Measurement Techniques Discussions

To investigate the similarities and contrasting features associated with various contributions to the cloud reflectivity profile, it is important to explore further the case of Figure 1. Statistical de-correlation times associated with three types of echo have been computed for their identification and separation. Both the cloud at ~3.7 km narrow region and insect returns below ~ 1.5 km in Figure 3 are evident above the maximum noise level. Both cloud and insect parts of the Z profiles are expanded to allow for review of the mean (Figure 3b and 3d) and standard deviation (σ; Figure 3c and 3e) of Z for every set of consecutive 15 profiles. Figure 3b shows the patterns of the seven mean cloud reflectivity profiles are organized and more consistent or correlated to one another during 105 seconds, this is in comparison to less organized reflectivity profiles due to insects that are much less consistent or correlated with one another in figure 3d. Moreover, the corresponding seven σ profiles show differences for cloud that is less than 1.5 σ (figure 3c). By comparison differences in profiles due to insects are more than 4.0 σ most of the time (figure 3e). It is seen that the mean cloud reflectivity peak values gradually extend from 3.7 to 3.8 km where the corresponding standard deviation values are less than 1σ. In order to further test the minimum de-correlation time associated with cloud and biota, the averaging time is reduced to a set of 5 profiles (5 sec) with the same data (see Figure 4). In this case also, Figure 4c depicts σ for all the seven mean cloud reflectivity profiles are below 1.5 with peak <1σ. This manifests that volumetric distribution nature of cloud particles is statistically more homogeneous or show less dispersion. However, Z values associated with biota show random behavior with significant dispersion >1.5σ (Figure 4e). This high dispersion in the Z values infers that the echo due to biota de-correlates quickly within ~5 second time interval (see Figure 4d-4e). It is seen from Figure 3 that for vertical levels from 0.9 km to 1.5, the sharp peaks in reflectivity profiles and strong dispersion of > 3σ are associated with the return from biota. This is attributed mostly to the observed intermittent point target nature of insect echoes plausibly due to the rambling or meandering motion of insects within the radar sampling volume. Moreover, the inherent radar system noise (random in nature) dispersion is observed to be in between the cloud and biota (1.5-3.0 σ). It is evident from the top panels of Figure 3-4 that cloud reflectivity profiles show relatively consistent trend and correlation among the contiguous mean profiles computed from the set of 15 Z profiles than computed from the 5 profiles. This may be mainly due to the homogeneities or in-homogeneities associated within the chosen data sets those are independent to one and another. Therefore, in order to preserve the real time sequence of observations for the study of cloud evolution as well as to recover underlying smooth trends pertinent to natural clouds, a four-point moving or running average is applied on the time series of Z data instead of deriving a simple average. The four seconds is the optimal moving average time for yielding the best cloud results (Figure 5) by characterizing the cloud to insect echoes coherent to incoherent property during the moving average period. By this four point running average, insect echo become incoherent due to its short de-correlation period (~4 sec) whereas those echoes de-correlating over longer periods indicate the presence of clouds. To understand the degree of dispersion, along with σ the absolute deviations in mean and median values have also been analyzed. Their relation with σ is seen to be as mean absolute deviation slightly smaller than σ as σ/1.253 where as median absolute deviation smallest as σ/1.483. This work makes use of the statistical mean and σ but using above relation one can relates the present results with other statistical central tendencies of data distribution. Next, the filtering of noise and insects from the presence of cloud using the cloud radar reflectivity profile will be explored. The segregation has been carried out using theoretical

Atmos. Meas. Tech. Discuss., https://doi.org/10.5194/amt-2017-254
Manuscript under review for journal Atmos. Meas. Tech.
Discussion started: 22 August 2017

Atmospheric Measurement Techniques Discussions

radar echo sensitivity curves and statistically computed echo de-correlation periods and finally tracking the cloud echo peak to its adjacent sides till it is close to the S1 profile for the cloud height. The above set of tasks, Theoretical Echo Sensitivity and observed Echo based Statistics for cloud height Tracking (TEST), is repetitively performed on the cloud radar Z measurements under an algorithm whose flowchart can be seen in Figure 6. The algorithm used in this work is named as TEST and can be summarized below:

1. Wherever the moving mean Z values in the profile are equal to or above the S5 can be qualified as cloud or insect. This step ensures removal of the system noise floor.
2. Those altitude regions of the qualified echo are then further scrutinized to identify clouds using the minimum thickness of greater than 100 m (to strictly avoid biota that are found to extend less than 2-4 height bins each of 25 m) and mean standard deviation below 1.5σ.
3. In order to keep the identified cloud's structure, intact, the identified cloud peak(s) are tracked back on either side (towards upper and bottom heights) up to around (preferably 1-2 dBZ) the mean noise profile S1.

It is interesting to note that the cloud echo regions are always stronger and above the mean noise fluctuations i.e., S1. Therefore at the left side of the curve, S0 to S1, always appears as a void region in the 2-dimentional reflectivity plot wherever there is a presence of cloud, no matter weak or strong (just below 4 km in the left panel of Figure 1 and 3). This causes sharp boundary gradients between cloud and noise in the vertical profiles of Z and hence with the corresponding σ. This can be used as a visual criterion for detection of cloud.

Figure 7 is similar to Figure 1 but it represents a multi layer pre-monsoon cloud system for the period 1200-1205 UT, 29 May 2014. Various labeled altitude regions (biota, noise and cloud) of the vertical reflectivity structure show typical mean features that can be broadly classified the returns into cloud and non-cloud (biota and noise) portion. Furthermore, Figure 7 shows the typical variety of cloud layers existing within the vertical structure of tropical cloud as well as morphological features pertinent to pre-monsoon thunderstorm activity. The cirrus layer at 12-14 km shows gradual structural change having peak reflectivity values of ~ 5 dBZ. Here, the high reflectivity values contribute to form single deep convective cloud by merging with the cloud layer that exists at lower heights.

Figure 8a and 8b reveal the reflectivity time series associated with the labeled non-cloud and cloud portion of Table 2 respectively. Noise and biota shows max 2 dB fluctuations around the 4-point-running mean reflectivity whereas for biota the max fluctuation is 3-5 dB (bold solid line). It can be understood that noise values increase gradually with altitude with σ values ~ 2.3 whereas sharp boundary gradients associated with biota and ragged shallow cloud regions (cloud 1&2 in Figure 7) also show higher σ values > 3. Stable or layer cloud regions (cloud 4 & 5 in Figure 7) show significantly standard deviation below 2σ. Further, it is interesting to examine the time series plots for the contrasting variations between the insects and noise and cloud regions with Figures 8a and 8b. The range of dBZ variability is 4-10 for insects and 2-4 for noise and for cloud that is less than 1 within an interval of 5-10 seconds. The corresponding variability in standard deviation (S.D) is observed to be 4-10 σ for insects, 1.5-3.5 σ

Atmos. Meas. Tech. Discuss., https://doi.org/10.5194/amt-2017-254
Manuscript under review for journal Atmos. Meas. Tech.
Discussion started: 22 August 2017

Atmospheric Measurement Techniques Discussions

for noise and ~ 1 σ for cloud (<1 σ for cloud peak) except for weaker cloud regions. These statistical characteristics of all types of observed cloud echoes have been tabulated in the Table 2.

Figure 9 demonstrates the application of the work presented here and illustrates the significant differences between the uncorrected (Figure 9a) and corrected (Figure 9b) reflectivity profiles. The peaks in frequency distribution of uncorrected cloud reflectivity profiles at just below -50 dBZ, in between -50 and -40 and just above -40 dB are the predominant contributions from noise (middle panel of Figure 9a). These noise regions bias severely the corresponding histogram frequency distribution at three different altitude levels that are associated with the Johnson's tri-modal cloud distribution (extreme right panel of Figure 9a). In order to infer the distribution of cloud reflectivity values in the various altitude regions pertinent to tri-modal cloud vertical structure (Johnson et al., 1999), the observed vertical structure is subdivided into warm or low (<3.6 km), mixed or mid (3.6 km ≥ altitude ≤8.6 km) and ice or high (>8.6 km) phase and/or level clouds. The plots of uncorrected reflectivity distribution clearly shows skewness towards lowest values of reflectivity (below -50dB, -40 dB and -30 dB for low, mid and high level respectively seen with right panels of Figure 9a). This is mainly due to the predominance of noise contribution except for the low cloud regions where the contribution of insects is also included. After applying the TEST algorithm the corrected reflectivity distribution peaks at -42dB, -35 dB and -22 dB for low, mid and high level respectively (right panel of Figure 9b) reflects the actual scenario of the cloud system. This method is simple and has potential to bring out the statistically significant micro- and macro-physical characteristics from meteorological information (i.e., cloud) and hence for better characterization of the cloud vertical structure over a region.

In order to test the merit of the current algorithm on filtering out the non-meteorological contribution with Z profile, the parametric thresholds on Pulse-Pair (PP) processed Z and few polarimetric variables profiles of the cloud radar measurements have also been considered in place of usual Fast Fourier Transformation (FFT) process. The FFT process is capable to provide only polarimetric parameter, i.e., linear depolarization ratio (LDR). Figure 10 is similar to the Figure 1 that illustrates FFT (top) and PP (bottom) processed Z profiles on 28 Aug 2014 but are 15 minutes apart from one another (0415 and 0400 UT respectively) which causes some dissimilarities in the observed three layer cloud structure between the two plots (upper and lower panel). Minimum range of the noise floor in the Z profiles (2-D plot in the first panel) is seen to be grater for PP than FFT processing. The TEST algorithm performs in a similar way for both the FFT and PP processed Z profiles and is able to isolate the cloud structure as best as possible. Figure 11 explores further the polarimetric capability of the KaSPR in separating out the meteorological contribution with Z by using critical threshold on the PP-polarimetric measurements that correspond to the bottom panels of Figure 10. The top panels of Figure 11 stand for HTI plots of, three polarimetric parameters namely, LDR, Φ_{dp} and K_{DP}. Computation of LDR is inherently limited to the cross polar isolation of the radar system that is -27 dB for KaSPR. Hence, high LDR values above -17 dB are mostly seen with insect and low LDR values below -17 dB are seen with cloud. Low to lower LDR values (i.e., <-17 dB to -25 dB) are strictly confined within the peak values of co-polar reflectivity (> -10 dB) of cloud altitude regions, ~ 8-10 km. Except the inherent limitations associated with LDR, these results are in agreement with earlier reported results (e.g. Bauer-Pfundstein and Görsdorf, 2007 and

Atmos. Meas. Tech. Discuss., https://doi.org/10.5194/amt-2017-254
Manuscript under review for journal Atmos. Meas. Tech.
Discussion started: 22 August 2017

Atmospheric Measurement Techniques Discussions

Khandwalla et al., 2003). The LDR, Φ_{dp} and K_{DP} threshold values are set below -17 dB, 56^0 and -15^0 km^{-1} respectively, can be used to filter out biota from the corresponding Z profiles that are shown at lower panels of Figure 11. The threshold used for Φ_{dp} and K_{DP} are subjective depending on the observed case for better filtering of insects. These polarimetric threshold methods are although successful in filtering out the non-meteorological contributions but they are bound to sacrifice the weaker portion of the cloud where polarimetric computations are not perfect. Thus, polarimetric method is incapable to preserve the weaker portions of the whole cloud regions where the TEST method is noticed to perform better (bottom right panel of Figure 10). This further proves the efficiency of the proposed TEST method. This has implemented in the post-processing of high resolution reflectivity measurements. The method developed here is far simpler and provides a superior solution to filtering out signal due to noise and biota and preserve cloud data in the form of pure meteorological reflectivity measurements which can be used to infer the true characteristics of clouds.

Figure 12a demonstrates further application of the current work on filtered cloud reflectivity profiles (bottom plot) by considering the six hours evolution of variety of tropical cloud systems. On 21 May 2013, a typical convective cloud system present during pre-monsoon season was observed. This event is composed of three systems, first three hours (00:00-03:12 UT) shows stratiform cloud confirmed from bright band occurrence at an altitude of 4 km AGL, convective system around 0500 UT, which is a cumulus congestus initially , and above it cirrus (ice) cloud in the altitude range of 13-14 km. The screened out reflectivity profile can therefore be utilized to fully characterize the tri-modal cloud episode as shown in Figure 12b. The mean reflectivity profile with standard deviation bars reveals the nature of important phase change regions associated with cloud vertical structure. The change in cloud processes in the cloud vertical structure is closely associated with the phase of cloud water that is strongly linked with the predominant change of temperature.

4.0 Summary and Conclusions

High resolution vertically oriented reflectivity measurements of cloud radar are solely potential to understand the cloud vertical structure after segregate the meteorological and non-meteorological contributions with it. Theoretical noise equivalent reflectivity curves are used to remove the system noise. The simple statistical variance of continual radar echoes show the contrasting different characteristic of signals like high dispersion (more than 2σ) is associated with the highly spurious and intermittent echoes of insects and low dispersion (less than 1σ) is associated with coherent nature of echoes of cloud hydrometeors and for noise it is 1.5-3.0 σ. Furthermore, these characteristic features are mainly used to demarcate the returns of cloud hydrometeor to those from insects and noise. Running mean and standard deviation of reflectivity profiles for ~4-5 seconds that works well to filter out all non-hydrometeor returns. In this way, the de-correlation period associated with biota helps in identifying and filtering out the insect returns. The proposed TEST algorithm evaluates the observed cloud radar reflectivity profiles with combined theoretical radar sensitivity curves and statistical variance of radar echo and then tracks the cloud peak at either side to obtain the complete cloud height profile. In case of azimuth and elevation radar surveillance scans (PPI and RHI, for example), there is a regular change in the radar sampling area that disables to have exclusive set of

measurements required to perform the TEST method. But this method is advantageous and easily adaptable for better characterization of any high-resolution vertical profile measurements. The robustness of TEST is also proved through polarimetric methods and found that it works much better, particularly in the weak cloud region, at the cloud radar frequencies. Such scrutinized reflectivity profiles has been further utilized to investigate the important CVS pertinent to the various phases of the Indian Summer Monsoon with the aim of improved prediction. Hence, the proposed TEST algorithm is able to extract the possible unbiased meteorological cloud vertical structure information with the cloud profiling radar. This enables carrying out the pragmatically effective research investigations on the seasonal and epochal tropical cloud characteristics.

Acknowledgements: IITM is an autonomous organization that is fully funded by MOES, Govt. of India. The authors are thankful to Director, IITM not only for his whole hearted support for establishing the radar programme but also for monitoring and acting as a source of inspiration to promote this research to the next level. The authors are highly indebted to Dr Ernest Raj and all those who were involved and helped in setting up the IITM's Cloud Radar Facility, KaSPR as well as KaSPR design and development which was done at M/s Prosensing, USA. The radar data supporting this article can be requested from the corresponding author (kalapureddy1@gmail.com).

Reference:

Alberoni, P. P., Ducrocq, V. , Gregoric, G., Haase, G., Holleman, I., Lindskog, M., Macpherson, B., Nuret, M., and Rossa, A.: Quality and Assimilation of Radar Data for NWP–A Review, COST 717 document, ISBN 92-894-4842-3, 38, 2003.

Bauer-Pfundstein, M. R., and Görsdorf, U.: Target separation and classification using cloud radar Doppler-spectra, paper presented at the 33rd International Conference on Radar Meteorology, Am. Meteorol. Soc., Cairns, Australia, 6 – 10 Aug, 2007

Chandrasekar, V., Keränen, R., Lim, S., and Moisseev, D.: Recent advances in classification of observations from dual polarization weather radars, Atmos. Res., 119, 97–111, 2013.

Cho, Y.-H., Lee, G. W., Kim, K.-E., and Zawadzki, I.: Identification and removal of ground echoes and anomalous propagation using the characteristics of radar echoes, J. Atmos. Ocean. Tech., 23, 1206–1222, 2006.

Doviak, R. J. and Zrni´c, D. S.: Doppler Radar and Weather Observations, Academic press, London, UK, 1984.

Dufton, D. R. L. and Collier, C. G.: Fuzzy logic filtering of radar reflectivity to remove non-meteorological echoes using dual polarization radar moments, Atmos. Meas. Tech., 8, 3985–4000, 2015.

Frisch, A. S., Fairall, C. W., and Snider, J. B.: Measurement of stratus cloud and drizzle parameters in ASTEX with a Ka-band Doppler radar and a microwave radiometer. J. Atmos. Sci., 52, 2788–2799, 1995.

Gourley, J. J., Tabary, P., and Parent du Chatele,t J.: A fuzzy logic algorithm for the separation of precipitating from non-precipitating echoes using polarimetric radar observations, J. Atmos. Ocean. Tech., 24, 1439–1451, 2007.

Hajovsky, R. G., Deam, A. P., and LaGrone, A. H.: Radar Reflections from insects in the lower atmosphere, IEEE Transactions on Antennas and Propagation, M-4 4(2), 224_227, 1966.

Hardy, K. R., Atlas, D., and Glover, K. M.: Multiwavelength backscatter from the clear atmosphere, J. Geo. Res.,7 1(6), 1537-1552, 1966.

Harrison, D. L., Driscoll, S. J., and Kitchen, M.: Improving precipitation estimates from weather radar using quality control and correction techniques, Meteorol. Appl., 7, 135–144, 2000.

Harrison, D. L., Georgiou, S., Gaussiat, N., and Curtis, A.: Longterm diagnostics of precipitation estimates and the development of radar hardware monitoring within a radar product data quality management system, Hydrolog. Sci. J., 59, 1277–1292, 2014.

Hogan, R. J., Gaussiat, N., and Illingworth, A. J.: Stratocumulus liquid water content from dual-wavelength radar, J. Atmos.Ocean. Tech., 22, 1207–1218, 2005.

Hurtado, M., and Nehorai, A.: Polarimetric detection of targets in heavy inhomogeneous clutter, IEEE Trans. on Signal Processing, Vol. 56, 1349-1361, 2008.

Johnson, R.H., Rickenbach T.M., Rutledge S.A., Ciesielski P.E., and Schubert W.H : Trimodal characteristics of tropical convection, J. Climate, 12, 2397-2418, 1999.

Khandwalla, A., Sekelsky, S., and Quante, M.: Algorithms for filtering insect echoes from cloud radar measurements, Thirteenth ARM Science Team Meeting Proceedings, Broomfield, Colorado, 2003.

Kollias, P., and Albrecht, B. A.: The turbulent structure in a continental stratocumulus cloud from millimeter wavelength radar observations, J. Atmos. Sci., 57, 2417–2434, 2000.

Lhermitte, R. M: Probing air motion by Doppler analysis of radar clear air returns, J. Atmos. Sci., 23, 575–591, 1966.

Lhermitte R.: A 94-Ghz Doppler Radar for Cloud Observation, J. Atmos.Ocean. Tech., 4,36-48,1987.

Luke, E.P., Kollias, P., and Johnson, K. L.: A Technique for the Automatic Detection of Insect Clutter in Cloud Radar Returns, J. Atmos.Ocean. Tech., 25, 1498-1513, 2008.

Martner, B. E., and Moran, K. P.: Using cloud radar polarization measurements to evaluate stratus cloud and insect echoes, J. Geophys. Res., 106, (D5), 4891–4897, 2001.

Meischner, P., Collier, C., Illingworth, A., Joss, J., and Randeu, W.: Advanced Weather Radar Systems in Europe: The COST 75 Action, Bull. Amer. Meteor. Soc., 78, 1411–1430, 1997.

Mueller, E. A. and Larkin, R. P.: Insects observed using dualpolarization radar, J. Atmos. Ocean. Tech., 2, 49–54, 1985.

Mueller, E. A.: Differential reflectivity of birds and insects. Preprints, 21st Conf. on Radar Meteorology, Edmonton, AB, Canada, Amer. Meteor. Soc., 465–466, 1983.

Nguyen, C. M., Moisseev, D. N., and Chandrasekar, V. : A parametric time domain method for spectral moment estimation and clutter mitigation for weather radars, J. Atmos. Ocean. Tech., 25, 83–92, 2008.

Sassen, K., Mace, G. G., Wang, Z., Poellot, M. R., Sekelsky, S. M., and McIntosh, R. E.: Continental stratus clouds: A case study using coordinated remote sensing and aircraft measurements, J. Atmos. Sci., 56, 2345–2358, 1999.

Sekelsky, S. M., Li, L., Calloway, J., McIntosh, R. E., Miller, M. A., Clothiaux, E. E., Haimov, S., Mace, G. C., and Sassen, K.: Comparison of millimeter-wave cloud radar measurements for the fall 1997 cloud IOP, Proceedings of 8th ARM Science Team Meeting, 671–675, Dep. of Energy, Tucson, Ariz, 1998.

Steiner, M. and Smith, J.: Use of three-dimensional reflectivity structure for automated detection and removal of nonprecipitating echoes in radar data, J. Atmos. Ocean. Tech., 19, 673–686, 2002.

Teschke, G., Gorsdorf, U., Korner, P., and Trede, D.: A new approach for target classification of Ka-band radar data, Fourth European Conference on Radar in Meteorology and Hydrology (ERAD), Barcelona, 2006.

Torres, S. M. and. Zrni´c, D. S: Ground clutter canceling with a regression filter, J. Atmos. Ocean. Tech., 16, 1364–1372, 1999.

Unal, C.: Spectral Polarimetric Radar Clutter Suppression to Enhance Atmospheric Echoes J. Atmos.Ocean. Tech., 1781-1797, 2009.

Warde, D. A. and Torres, S. M.: Automatic detection and removal of ground clutter contamination on weather radars, Proc. 34th Conference on Radar Meteorology, Williamsburg, VA, USA, AMS, P10.11, 2009.

Zhang, P., Ryzhkov, A. V., and Zrnic, D. S.: Observations of insects and birds with a polarimetric prototype of the WSR- 88D radar, Preprints, 32d Int. Conf. on Radar Meteorology, Albuquerque, NM, Amer. Meteor. Soc., CD-ROM, P6.4, 2005.

Zrnic´, D. S. and Ryzhkov, A. V.: Observations of insects and birds with a polarimetric radar, IEEE Trans. Geosci. Remote Sens., 36, 661–668, 1998.

Atmos. Meas. Tech. Discuss., https://doi.org/10.5194/amt-2017-254
Manuscript under review for journal Atmos. Meas. Tech.
Discussion started: 22 August 2017

Atmospheric Measurement Techniques Discussions

Figure Captions

Figure 1. (a) Vertical looking cloud radar measured sample ten reflectivity height profiles on 27 April 2014 during 2303-2308 UT. S0 to S5 are the theoretical noise equivalent reflectivity curves with their respective threshold values in bracket. HTI plot of (b) the same reflectivity profile for the duration of 306 sec (c) screened out reflectivity profile for the receiver noise floor and the biota (insects) using running average constrained with standard deviation (d) constrained with NER (S5).

Figure 2. (left) Same as 1(a) but for 220 profiles. (right) HTI plot of Z profiles. Smoothly varying homogeneous cloud layer is at altitudes of 3.5-3.8 km and sharp, rounded and spurious kind of echoes below 2.7 km are due to biota.

Figure 3. (a) Same as 1(a) but for 105 profiles. (b) mean and (c) standard deviation of 15 profiles of Z pertinent to cloud height region (3.5-3.9 km) and (d) and (e) same as (b) and (c) but pertinent to insects height region (0.9-1.5 km).

Figure 4. Same as Figure 3 but for total duration 35 sec; the mean and standard deviation profiles are for every 5 second interval.

Figure 5. Same as Figure 3 but for total duration 10 sec; the mean and standard deviation profiles are for 4-point-moving average.

Figure 6. TEST algorithm flow chart that identifies and filter-out the insects and noise echoes for screening-out the cloud contributions with the Z measurements.

Figure 7. (a-c) Same as 1(a-c) but on 29 May 2014 during 1200-1205 UT for the duration of 306 sec. Statistics corresponds to the labels on the Z profile can be seen in Table 2.

Figure 8a. Time series of the mean and standard deviation (S.D) of Z for insects (bottom panels) and four noise floor regions as per Table 2. Bold solid lines are the 5-point-running mean over the actual time series data (lines with symbol).

Figure 8b. Same as Figure 8a but for the cloud regions as per Table 2.

Figure 9a. (Left panel) Uncorrected mean reflectivity profile on 29 May 2014 during 1200-1205 UT superimposed with curves S1 (dashed red line) and S5 (solid green line). Histogram of Z profile (Middle panel). (left three sub panels) for altitude regions of low (<3.6 km), mid (3.6 km>=ht<8.6 km) and high (>=8.6 km). The right sub panels each peak of histogram are mapped on to the corresponding three peaks with the whole vertical structure of Z. This infers the noise clearly suppresses the meteorological information.

Atmos. Meas. Tech. Discuss., https://doi.org/10.5194/amt-2017-254
Manuscript under review for journal Atmos. Meas. Tech.
Discussion started: 22 August 2017

Atmospheric Measurement Techniques Discussions

Figure 9b. Same as 9a but it is corrected by filtering out noise and biota. The correction applied to Z profile allows to pop-up the true meteorological cloud reflectivity distribution.

Figure 10. Same as 7 but for vertical looking KaSPR measurements at 0400 UT on 28 Aug 2014 using (top) FFT processing (bottom) 15 minutes prior one using PP processing. PP case will be used further to evaluate the polarimetric algorithm performance.

Figure 11. HTI plots of (top panel) LDR, Φ_{dp} and K_{DP} parameters pertinent to PP processed data of Figure 10 and (bottom panels) biota filtered reflectivity after applying corresponding polarimetric thresholds of the respective top panels.

Figure 12a. (Top) Same as Figure 7b (uncorrected) and (bottom) same as Figure 7c (corrected) but integrated for duration of 0000-0630 UT taken at an interval of ~ 15 minutes on 21 May 2013

Figure 12b. Same as Figure 9b but excluding middle panel for the corrected Z data of figure 12a.

Atmos. Meas. Tech. Discuss., https://doi.org/10.5194/amt-2017-254
Manuscript under review for journal Atmos. Meas. Tech.
Discussion started: 22 August 2017

Atmospheric Measurement Techniques Discussions

Table 1: KaSPR specifications

Radar specifications	value
RF output frequency	35.29 GHz
Peak power	2.1 kW
Duty cycle	5 % max.
Pulse widths (selectable)	3.3 ns (50-13000 ns)
Pulse compression ratio	1:10 (1-100)
Transmit polarization	H or V-pol linear; Pulse-to-pulse polarization agility
Receiver polarization	Simultaneous Co- and Cross-polarization linear
Receiver noise figures	2.8 dB min
Sensitivity at 5.0 km	-45 dBZ
Tx & Rx loses	1.15 & 0.3 dB
IF output to digital receiver	90 MHz
Antenna diameter	1.2 m
Antenna Beam width	0.5^0
Antenna gain (includes OMT loss)	49 dB
First side lobe level	-19 dBi min.
Cross-polarization isolation	-27 dB

Atmos. Meas. Tech. Discuss., https://doi.org/10.5194/amt-2017-254
Manuscript under review for journal Atmos. Meas. Tech.
Discussion started: 22 August 2017

Atmospheric Measurement Techniques Discussions

Table 2: Statistical mean and standard deviation of cloud radar reflectivity corresponds to the selected height regions, which are labeled, on the Figure 7.

Label	Mean Z for 305 sec (4 sec) dBZ	σ for 305 sec (4 sec)
Insects (1.2-1. 7 Km)	-54.1(-55.0)	4.08 (3.4)
Noise 1 (2.1-2.4 Km)	-52.9 (-52.4)	2.33 (1.9)
Noise 2 (5.9-6.2 Km)	-44.4 (-44.2)	2.22 (2.3)
Noise 3 (11.1-11.6 Km)	-39.1 (-39.1)	2.30 (2.2)
Noise 4 (14.7-15.2 Km)	-36.7 (-36.9)	2.29 (2.2)
Cloud 1 (3.7-3.9 Km)	-36.2 (-28.3)	5.99 (12.7)
Cloud 2 (4.8-5.1 Km)	-31.8 (-22.7)	5.54 (4.5)
Cloud 3 (6.8-7.2 Km)	-0.4 (0.3)	2.60 (3.5)
Cloud 4 (9.8-10.2 Km)	-10.9 (-9.9)	2.03 (3.1)
Cloud 5 (12.8-13.2 Km)	3.1 (1.4)	0.86 (1.0)

Atmos. Meas. Tech. Discuss., https://doi.org/10.5194/amt-2017-254
Manuscript under review for journal Atmos. Meas. Tech.
Discussion started: 22 August 2017

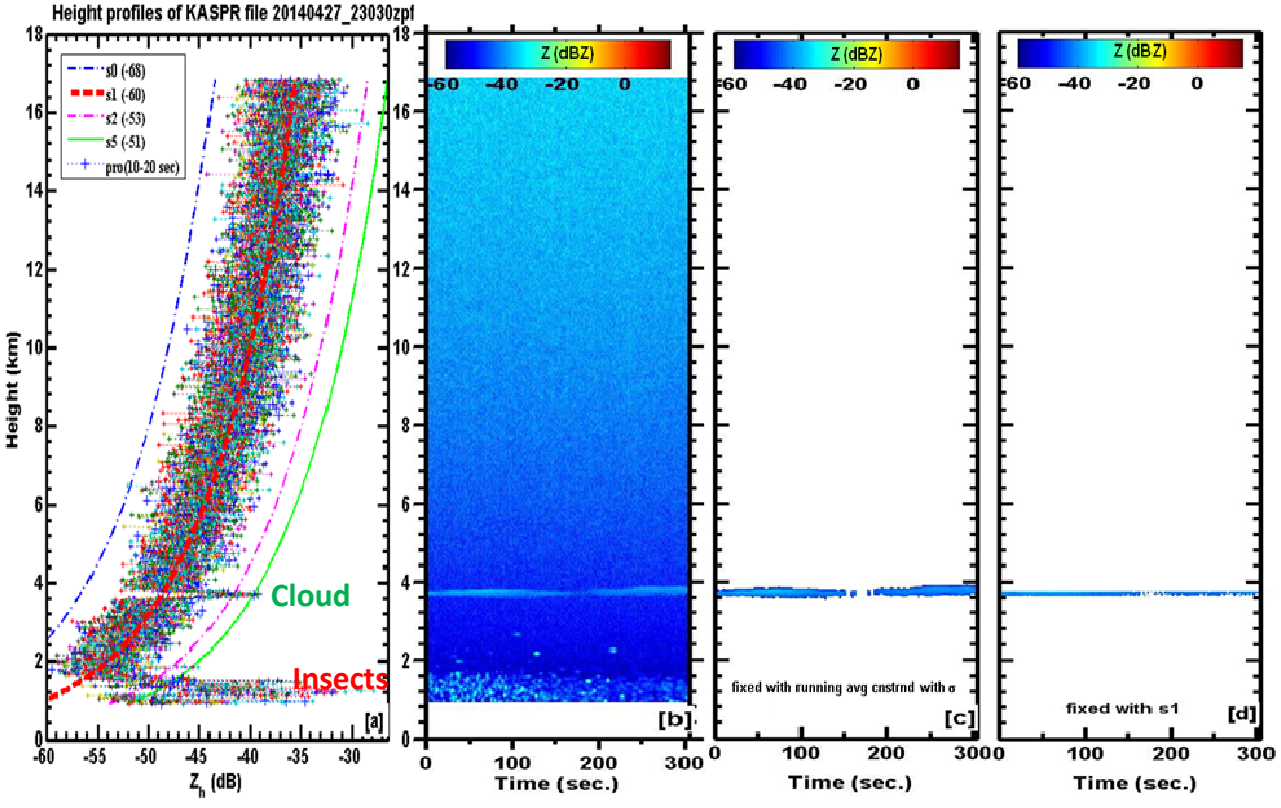

Figure 1: (a) Vertical looking cloud radar measured sample ten reflectivity height profiles on 27 April 2014 during 2303-2308 UT. S0 to S5 are the theoretical noise equivalent reflectivity curves with their respective threshold values in bracket. HTI plot of (b) the same reflectivity profile for the duration of 306 sec (c) screened out reflectivity profile for the receiver noise floor and the biota (insects) using running average constrained with standard deviation (d) constrained with NER (S5).

Atmos. Meas. Tech. Discuss., https://doi.org/10.5194/amt-2017-254
Manuscript under review for journal Atmos. Meas. Tech.
Discussion started: 22 August 2017

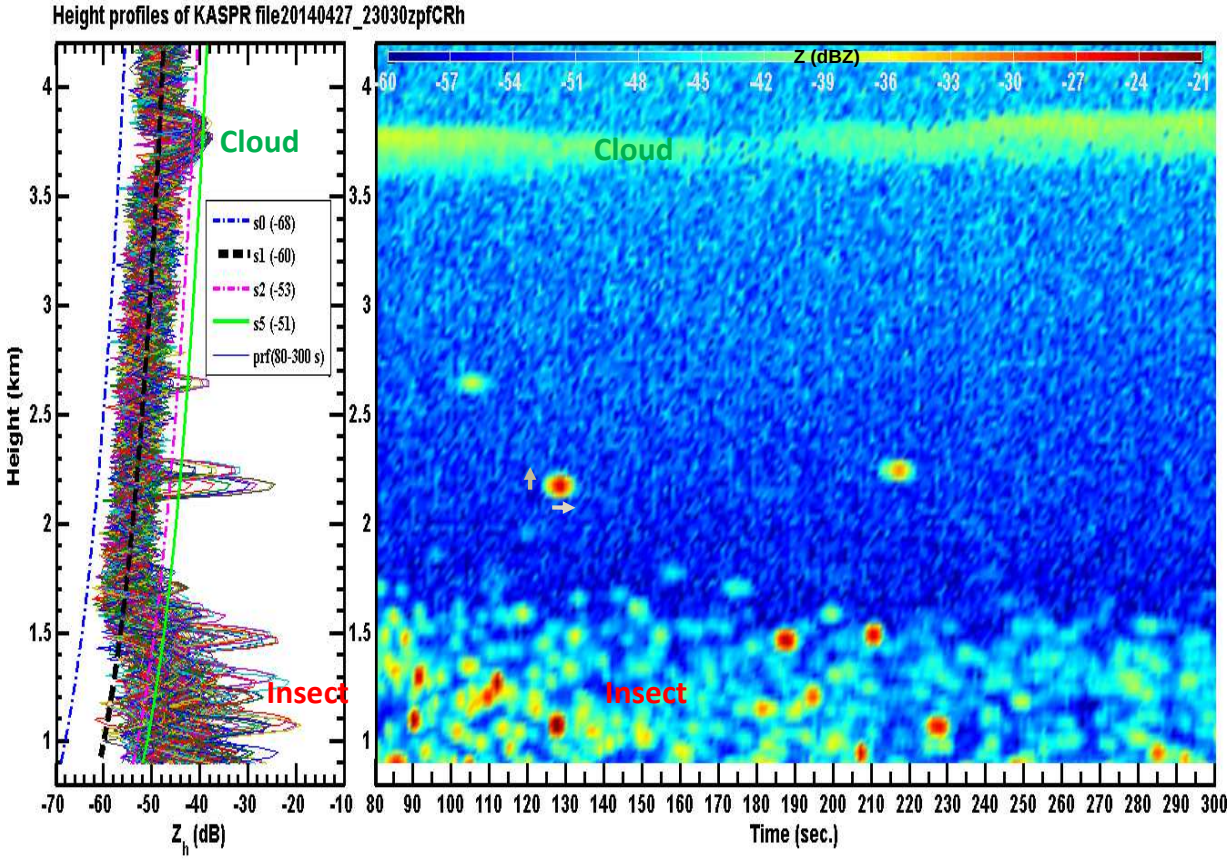

Figure 2: (left) Same as 1(a) but for 220 profiles. (right) HTI plot of Z profiles. Smoothly varying homogeneous cloud layer is at altitudes of 3.5-3.8 km and sharp, rounded and spurious kind of echoes below 2.7 km are due to biota.

Atmos. Meas. Tech. Discuss., https://doi.org/10.5194/amt-2017-254
Manuscript under review for journal Atmos. Meas. Tech.
Discussion started: 22 August 2017

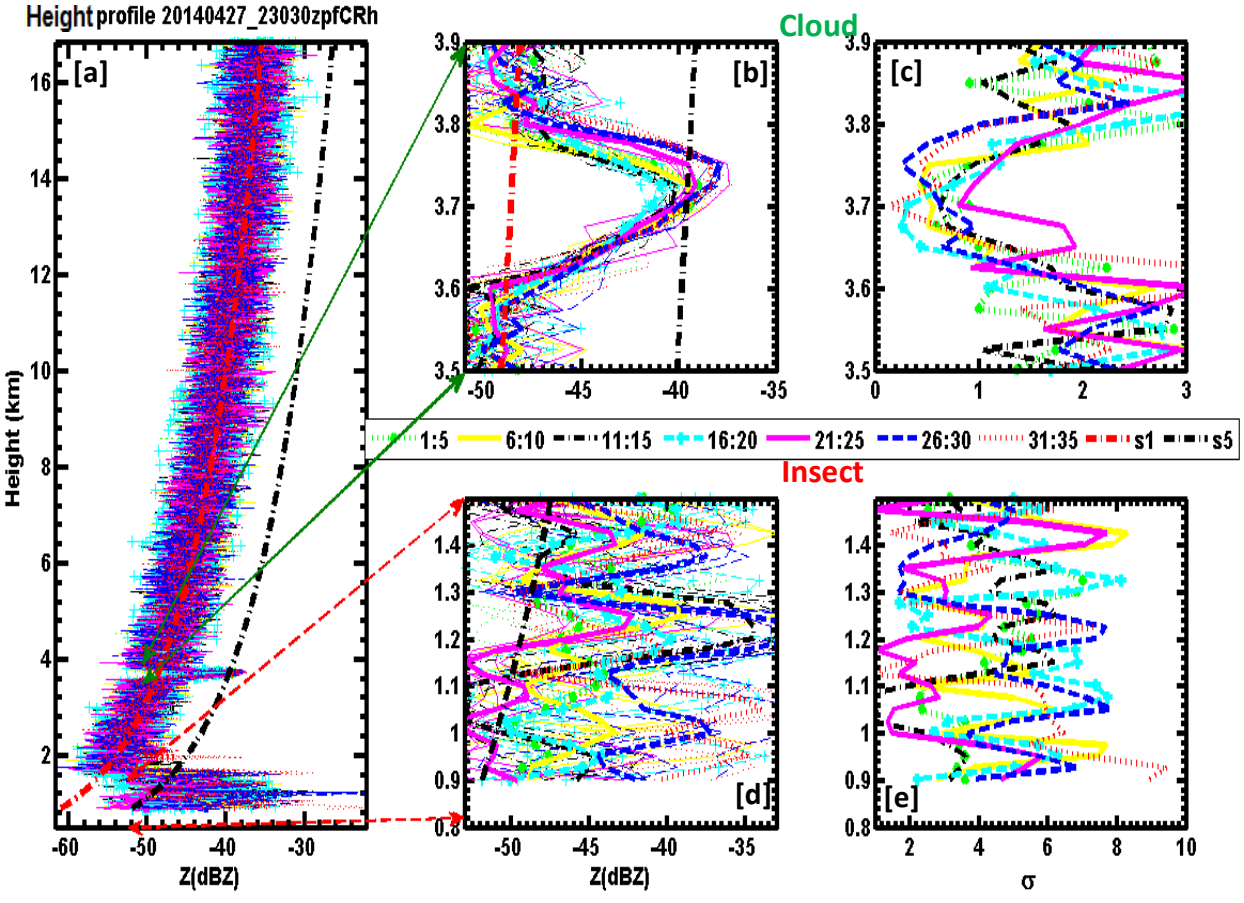

Figure 3: (a) Same as 1(a) but for 105 profiles. (b) mean and (c) standard deviation of 15 profiles of Z pertinent to cloud height region (3.5-3.9 km) and (d) and (e) same as (b) and (c) but pertinent to insects height region (0.9-1.5 km).

Atmos. Meas. Tech. Discuss., https://doi.org/10.5194/amt-2017-254
Manuscript under review for journal Atmos. Meas. Tech.
Discussion started: 22 August 2017

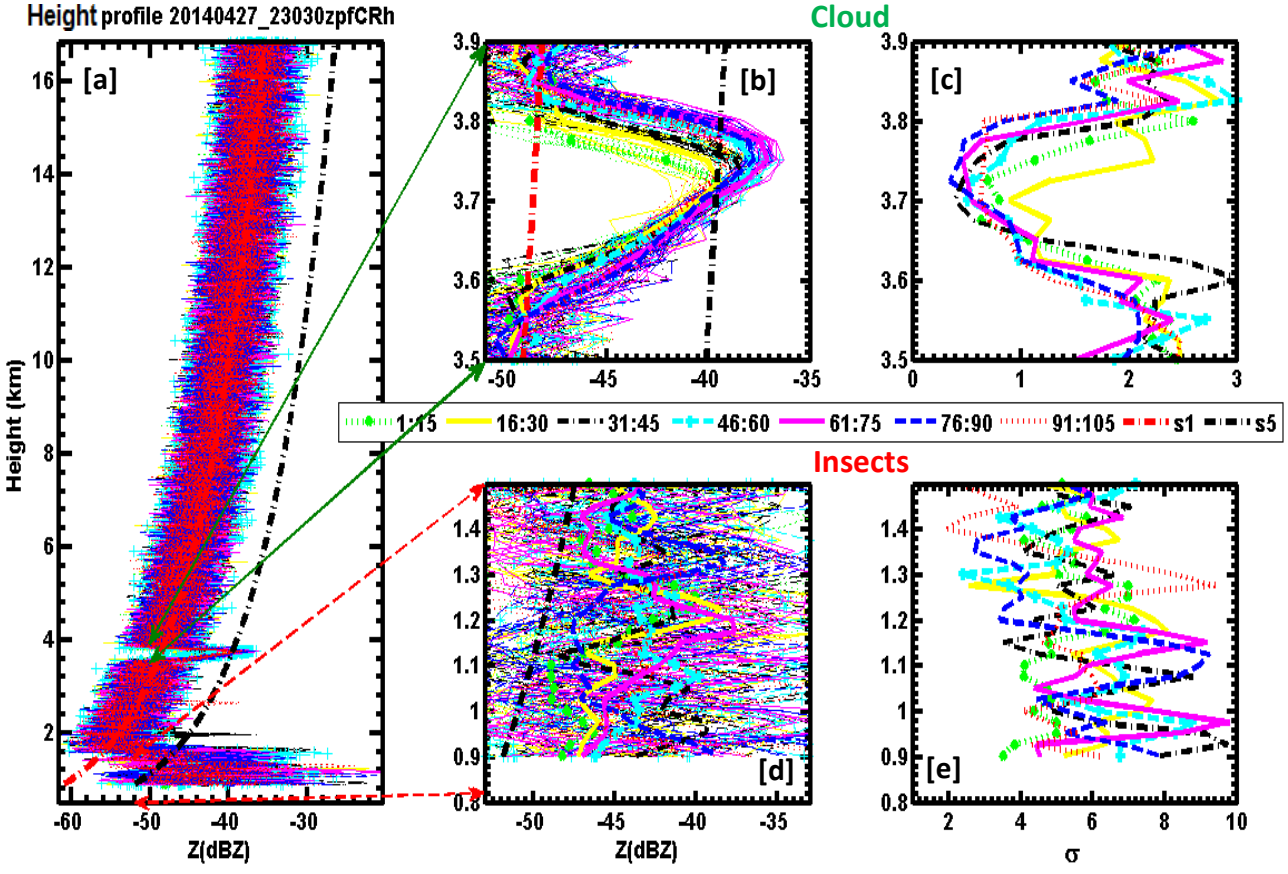

Figure 4: Same as Figure 3 but for total duration 35 sec; the mean and standard deviation profiles are for every 5 second interval.

Atmos. Meas. Tech. Discuss., https://doi.org/10.5194/amt-2017-254
Manuscript under review for journal Atmos. Meas. Tech.
Discussion started: 22 August 2017

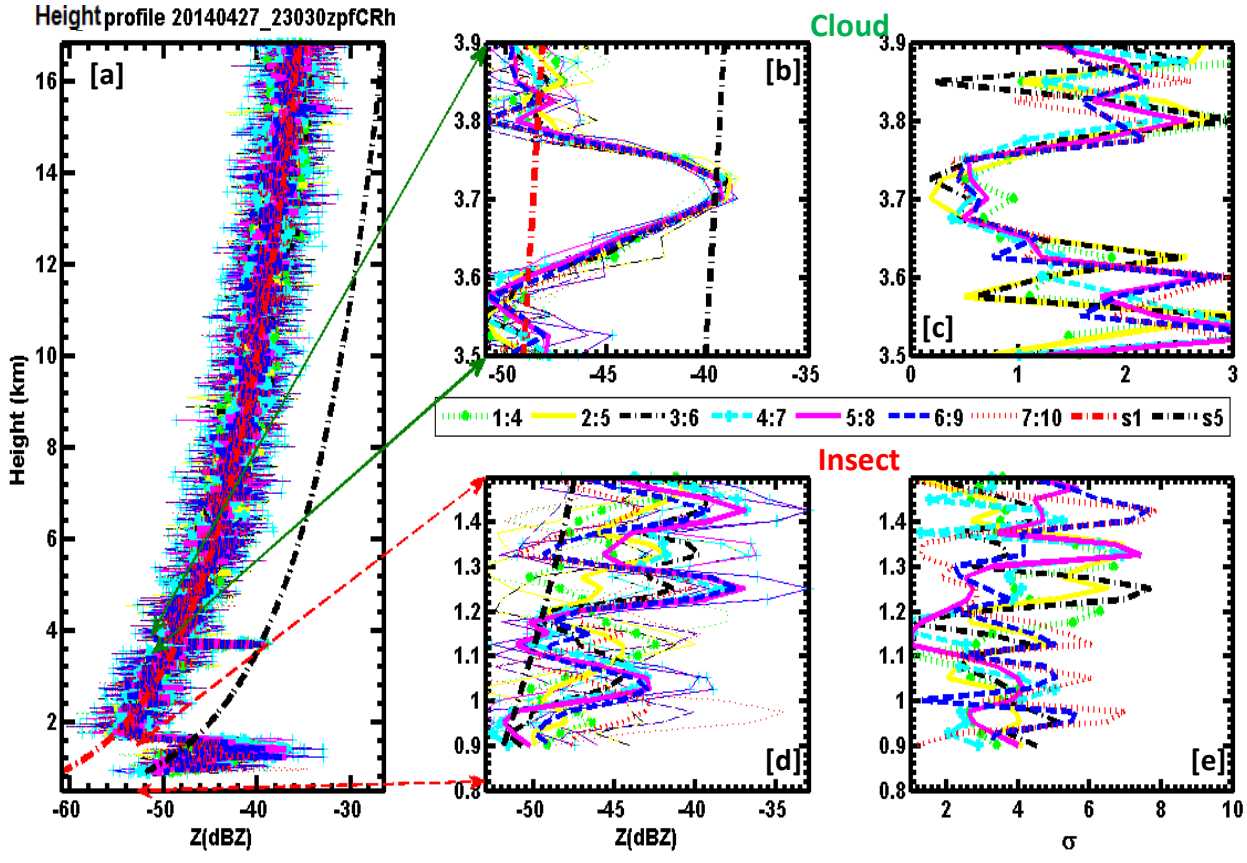

Figure 5: Same as Figure 3 but for total duration 10 sec; the mean and standard deviation profiles are for 4-point-moving average.

Atmos. Meas. Tech. Discuss., https://doi.org/10.5194/amt-2017-254
Manuscript under review for journal Atmos. Meas. Tech.
Discussion started: 22 August 2017

Atmospheric Measurement Techniques Discussions

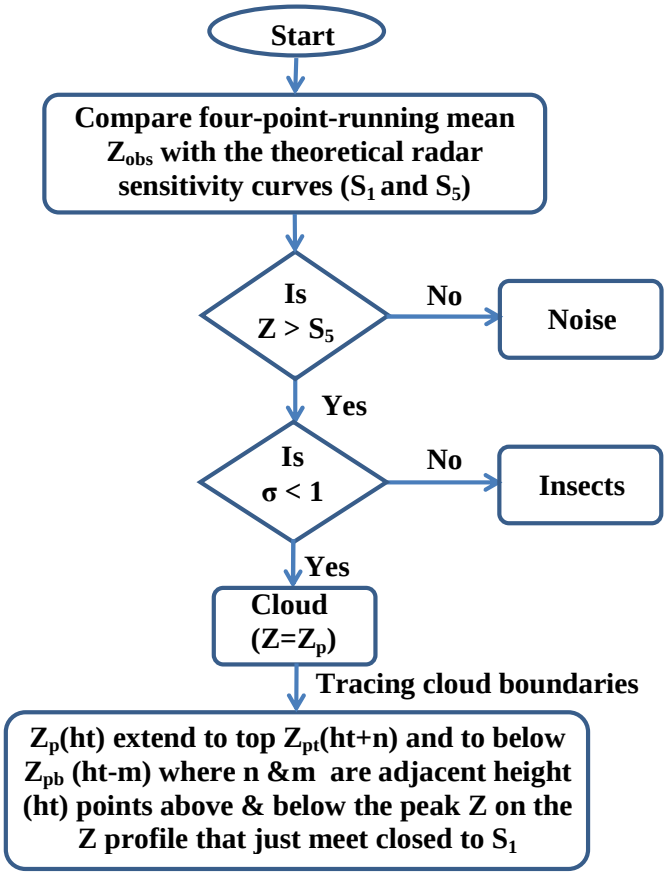

Figure 6: TEST algorithm flow chart that identifies and filter-out the insects and noise echoes for screening-out the cloud contributions with the Z measurements.

Atmos. Meas. Tech. Discuss., https://doi.org/10.5194/amt-2017-254
Manuscript under review for journal Atmos. Meas. Tech.
Discussion started: 22 August 2017

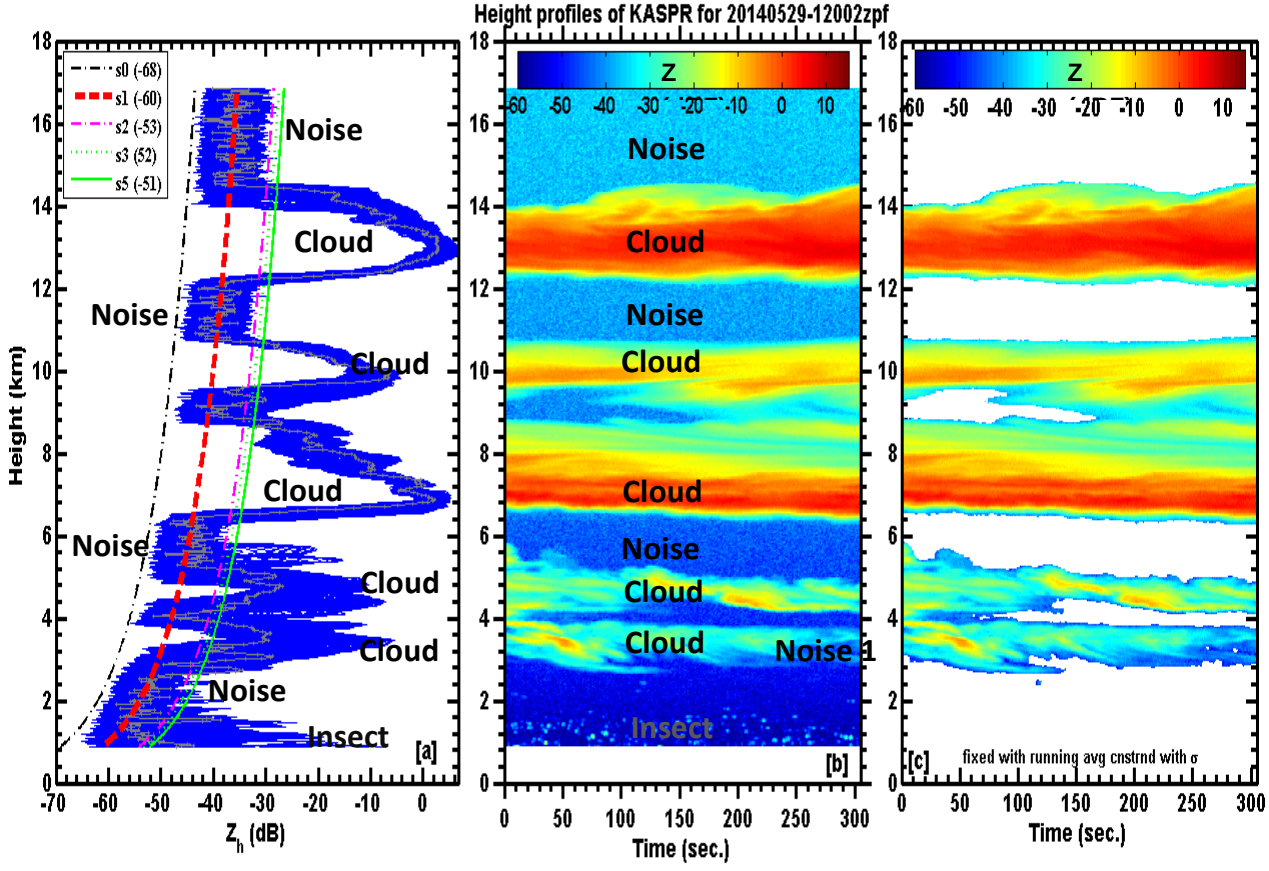

Figure 7: (a-c) Same as 1(a-c) but on 29 May 2014 during 1200-1205 UT for the duration of 306 sec. Statistics corresponds to the labels on the Z profile can be seen in Table 2.

Atmos. Meas. Tech. Discuss., https://doi.org/10.5194/amt-2017-254
Manuscript under review for journal Atmos. Meas. Tech.
Discussion started: 22 August 2017

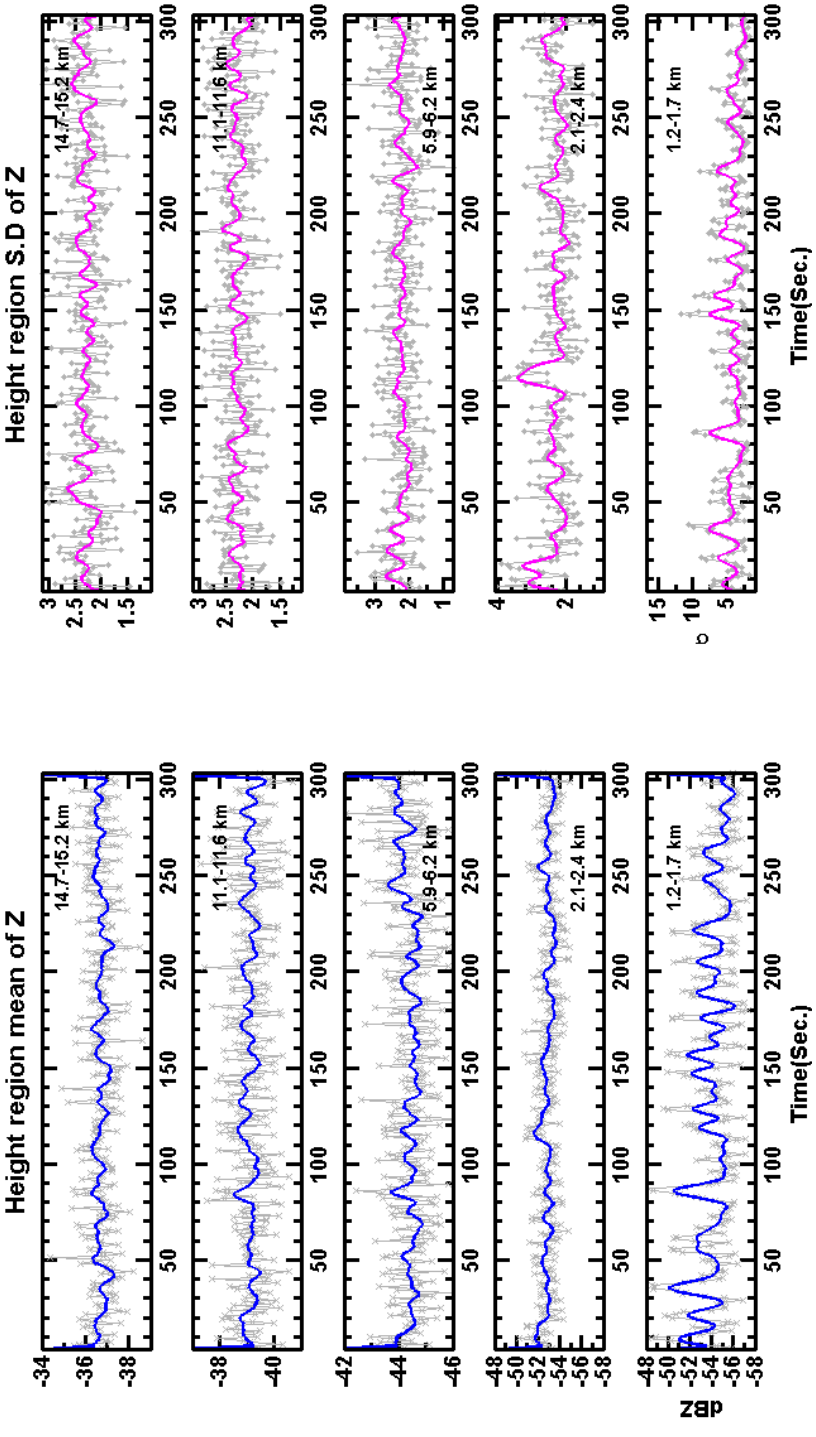

Figure 8a: Time series of the mean and standard deviation (S.D) of Z for insects (bottom panels) and four noise floor regions as per Table 2. Bold solid lines are the 5-point-running mean over the actual time series data (lines with symbol).

Atmos. Meas. Tech. Discuss., https://doi.org/10.5194/amt-2017-254
Manuscript under review for journal Atmos. Meas. Tech.
Discussion started: 22 August 2017

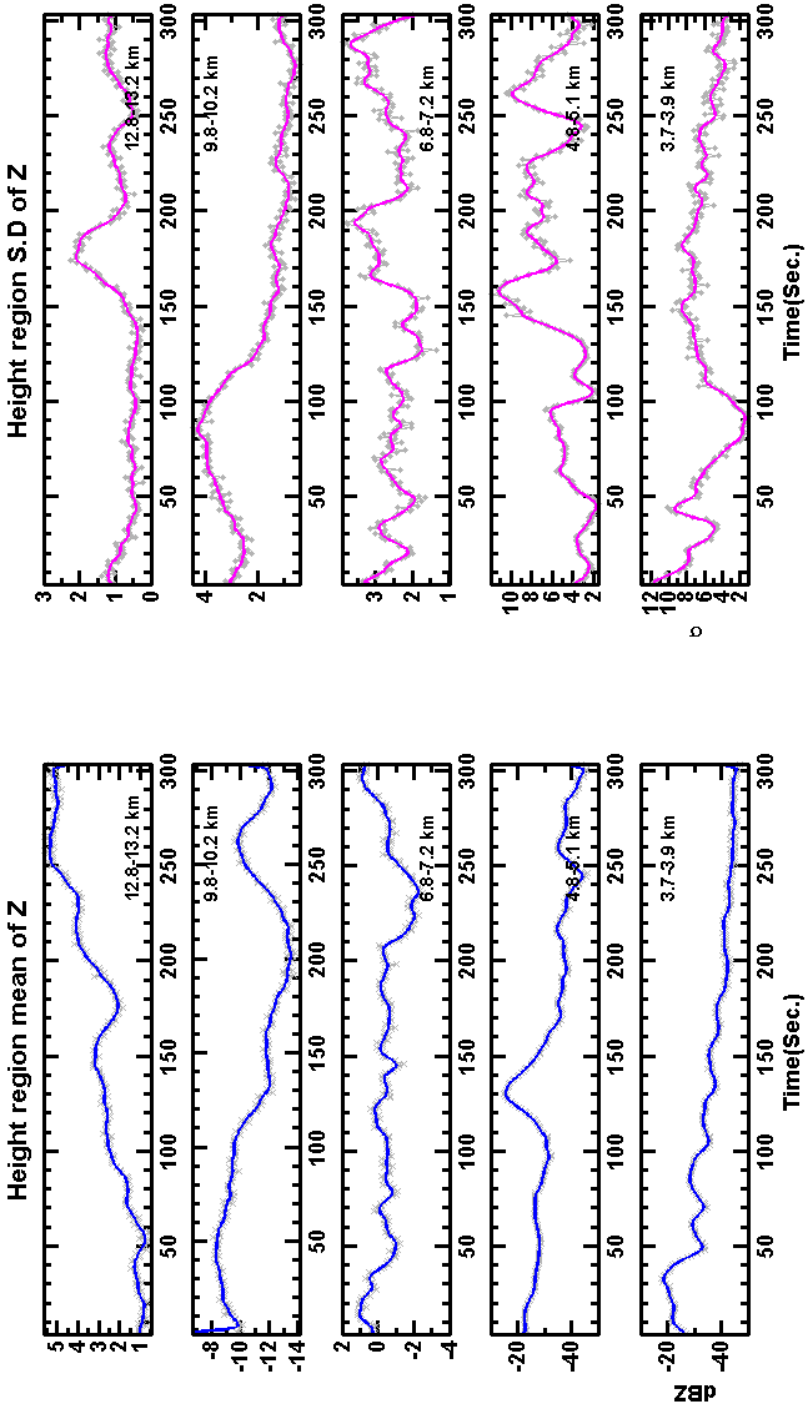

Figure 8b: Same as Figure 8a but for the cloud regions as per Table 2.

Atmos. Meas. Tech. Discuss., https://doi.org/10.5194/amt-2017-254
Manuscript under review for journal Atmos. Meas. Tech.
Discussion started: 22 August 2017

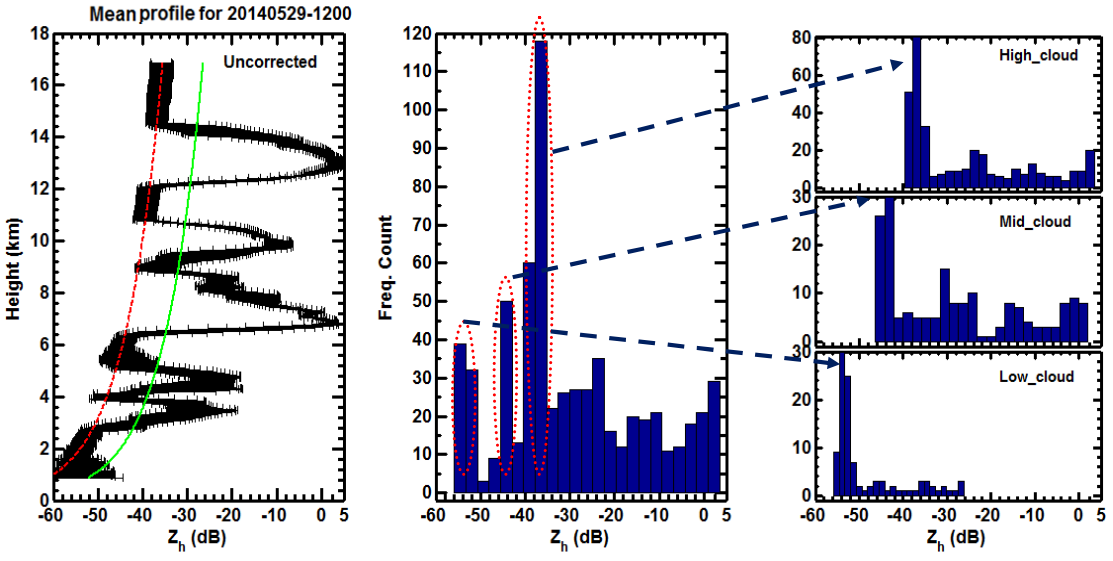

Figure 9a: (Left panel) Uncorrected mean reflectivity profile on 29 May 2014 during 1200-1205 UT superimposed with curves S1 (dashed red line) and S5 (solid green line). Histogram of Z profile (Middle panel). (left three sub panels) for altitude regions of low (<3.6 km), mid (3.6 km>=ht<8.6 km) and high (>=8.6 km). The right sub panels each peak of histogram are mapped on to the corresponding three peaks with the whole vertical structure of Z. This infers the noise clearly suppresses the meteorological information.

Atmos. Meas. Tech. Discuss., https://doi.org/10.5194/amt-2017-254
Manuscript under review for journal Atmos. Meas. Tech.
Discussion started: 22 August 2017

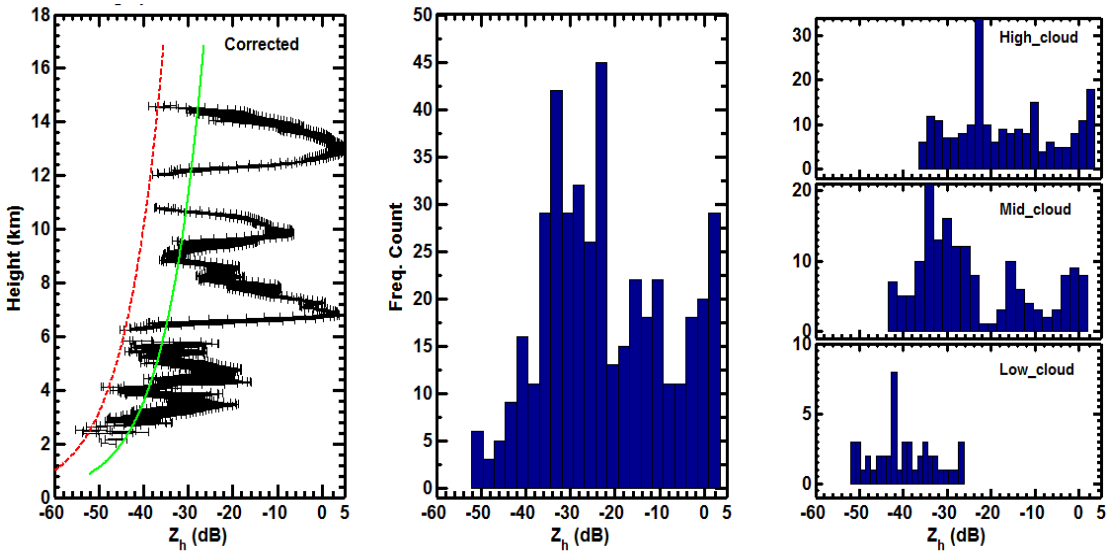

Figure 9b: Same as 9a but it is corrected by filtering out noise and biota. The correction applied to Z profile allows to pop-up the true meteorological cloud reflectivity distribution.

Atmos. Meas. Tech. Discuss., https://doi.org/10.5194/amt-2017-254
Manuscript under review for journal Atmos. Meas. Tech.
Discussion started: 22 August 2017

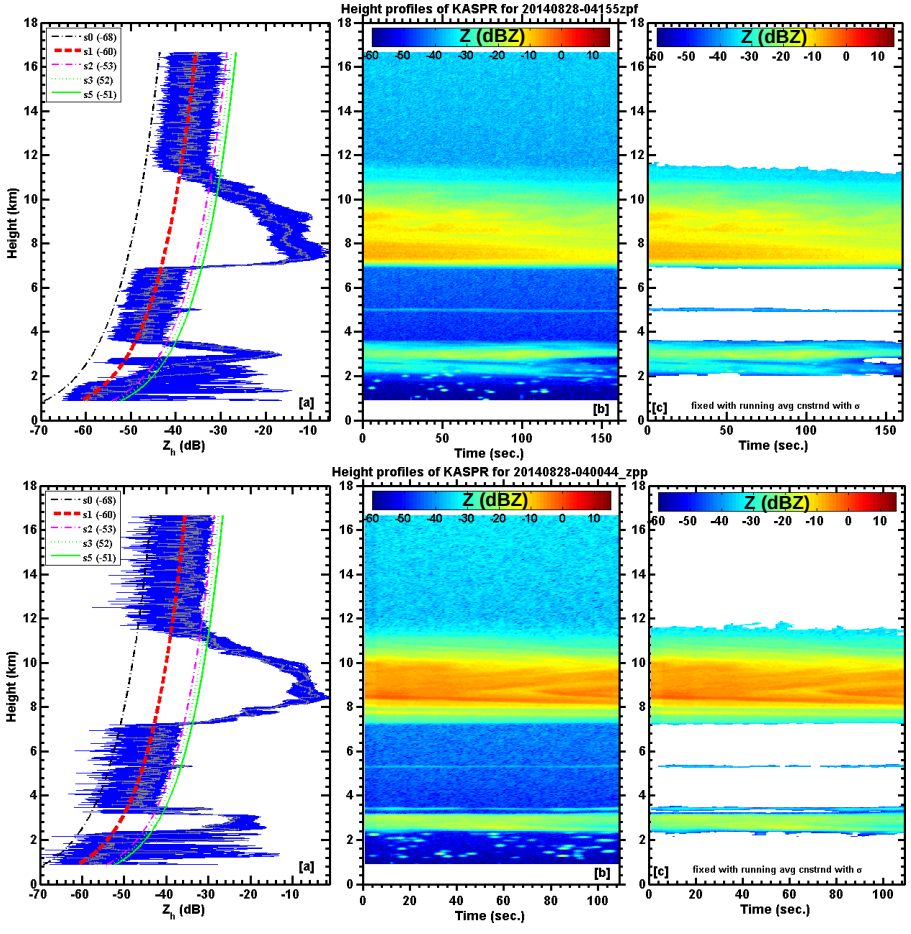

Figure 10: Same as 7 but for vertical looking KaSPR measurements at 0400 UT on 28 Aug 2014 using (top) FFT processing (bottom) 15 minutes prior one using PP processing. PP case will be used further to evaluate the polarimetric algorithm performance.

Atmos. Meas. Tech. Discuss., https://doi.org/10.5194/amt-2017-254
Manuscript under review for journal Atmos. Meas. Tech.
Discussion started: 22 August 2017

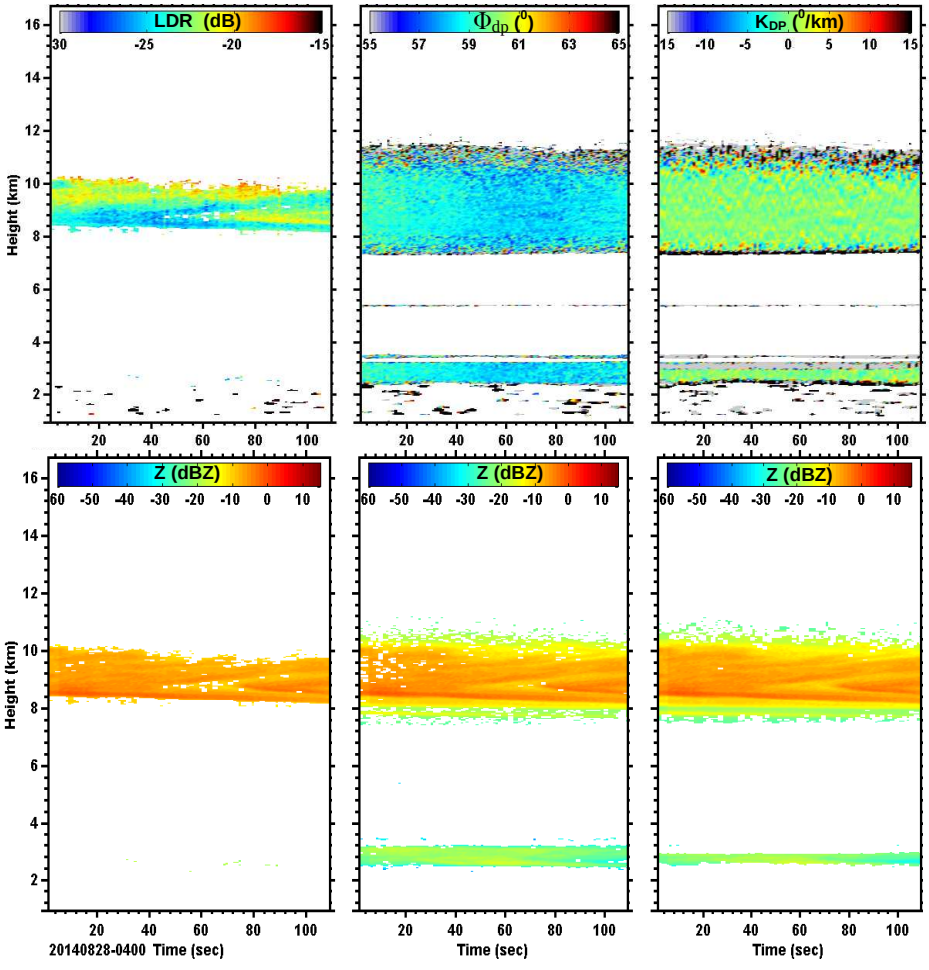

Figure 11: HTI plots of (top panel) LDR, Φ_{dp} and K_{DP} parameters pertinent to PP processed data of Figure 10 and (bottom panels) biota filtered reflectivity after applying corresponding polarimetric thresholds of the respective top panels.

Atmos. Meas. Tech. Discuss., https://doi.org/10.5194/amt-2017-254
Manuscript under review for journal Atmos. Meas. Tech.
Discussion started: 22 August 2017

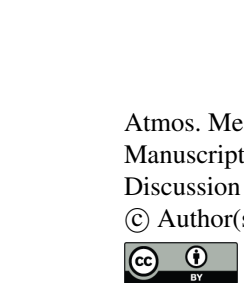

Atmospheric Measurement Techniques Discussions

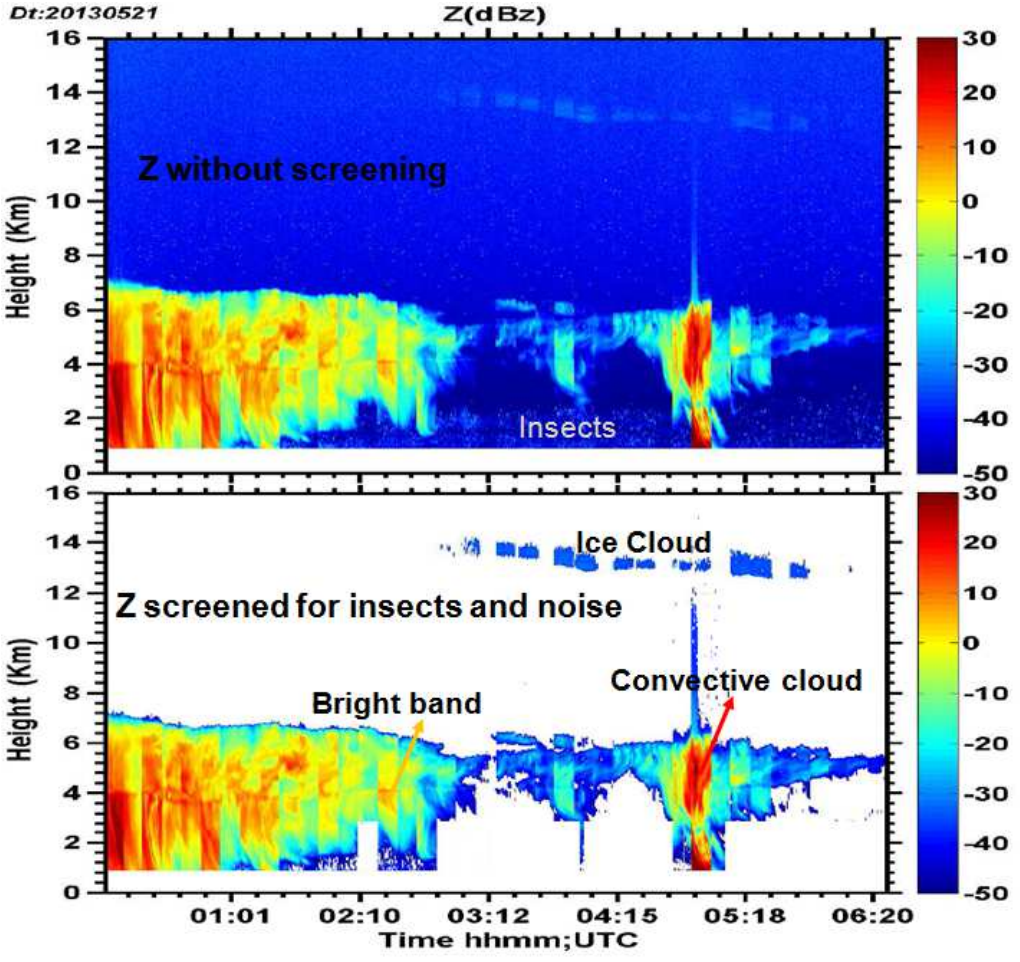

Figure 12a: (Top) Same as Figure 7b (uncorrected) and (bottom) same as Figure 7c (corrected) but integrated for duration of 0000-0630 UT taken at an interval of ~ 15 minutes on 21 May 2013

Atmos. Meas. Tech. Discuss., https://doi.org/10.5194/amt-2017-254
Manuscript under review for journal Atmos. Meas. Tech.
Discussion started: 22 August 2017

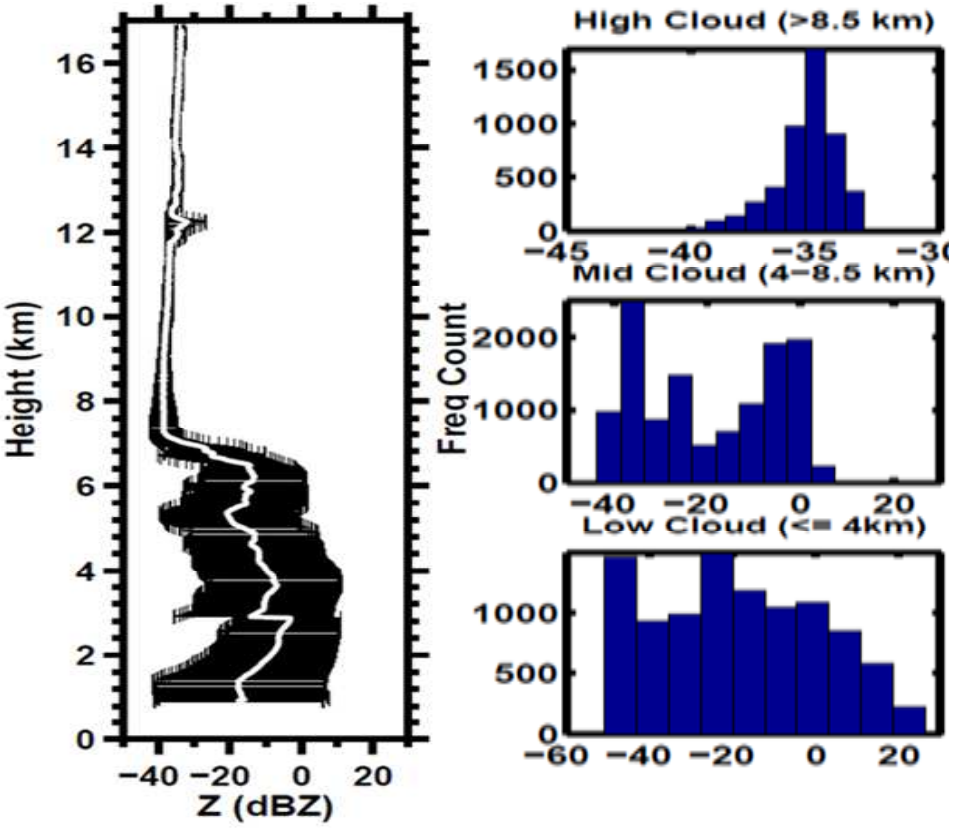

Figure 12b: Screened-out cloud radar reflectivity mean and standard deviation profile with the tri-model cloud reflectivity frequency distribution.

Atmos. Meas. Tech. Discuss., https://doi.org/10.5194/amt-2017-254
Manuscript under review for journal Atmos. Meas. Tech.
Discussion started: 22 August 2017

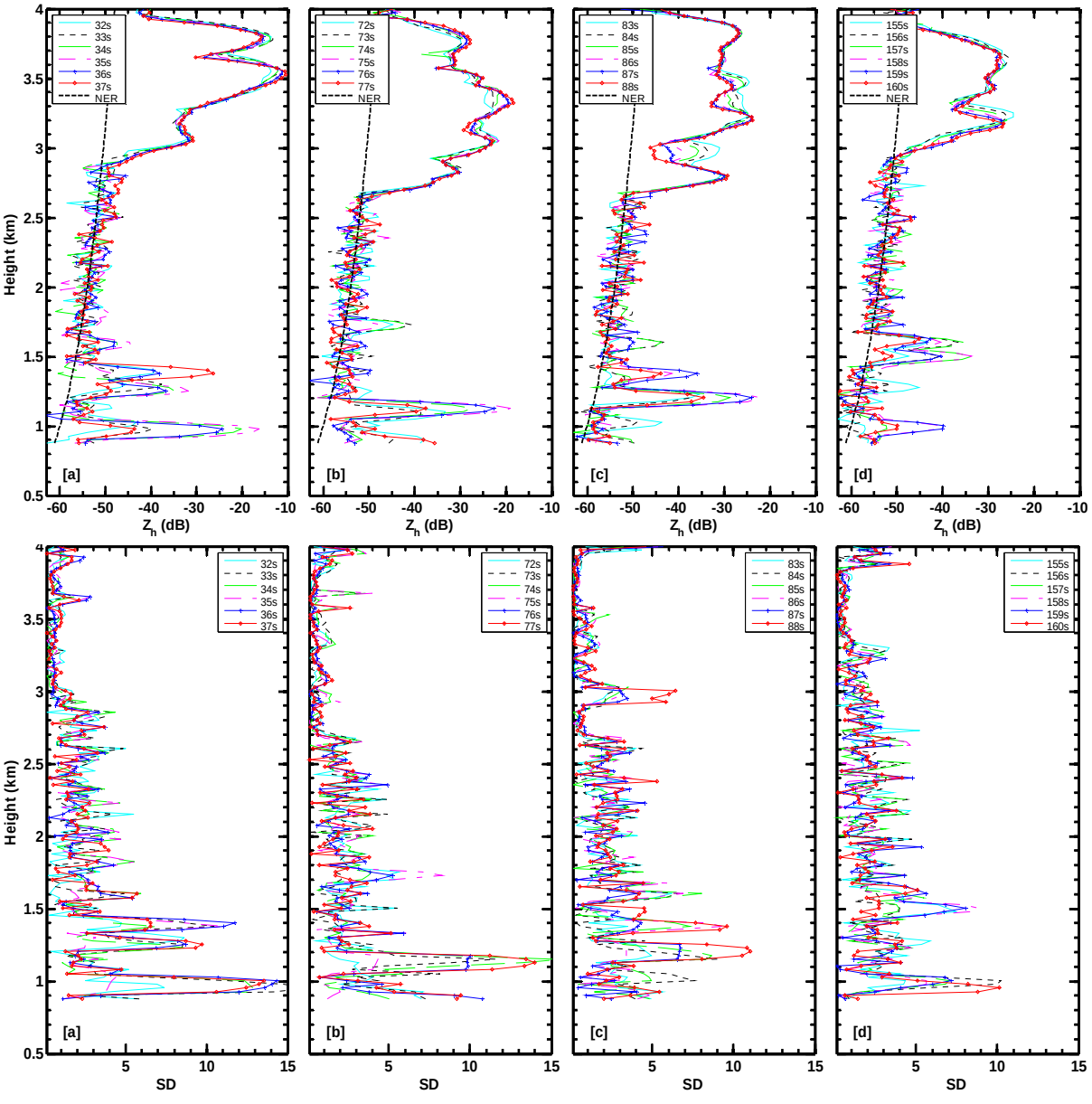

Figure A1: Instentaneous height profiles of Z during 1200-1205 UT on 29 May 2014 with centered numer profile notice to be the strong insect return identified with HTI plot of figure 4b. Bottom panesl correspond to standard devation (SD) from four point running average.

Atmos. Meas. Tech. Discuss., https://doi.org/10.5194/amt-2017-254
Manuscript under review for journal Atmos. Meas. Tech.
Discussion started: 22 August 2017

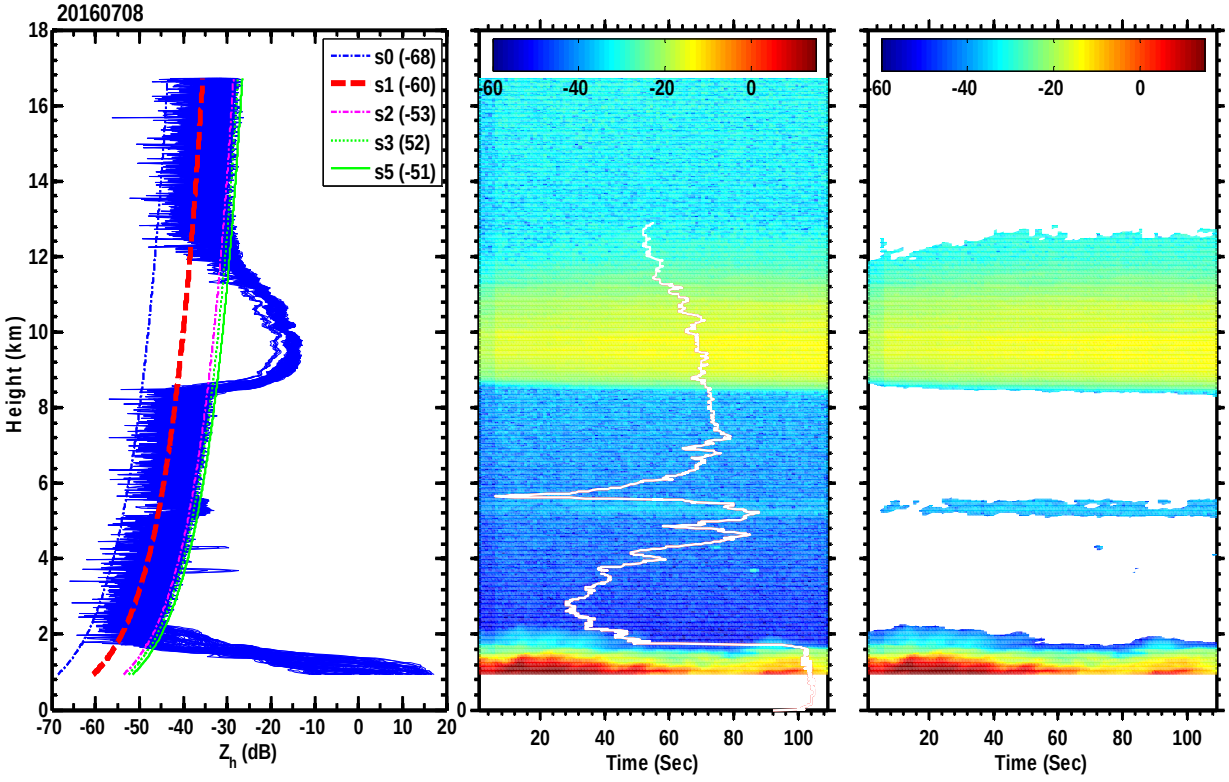

Figure A2: (Right-middle-left) Same as 1(a-c) but on 08 Jul 2016 during 0531 UT for the duration of 108 sec. S0-S5 are NER curves. Collocated GPS-RS relative humidity (%) profile had shown as while solid line in the middle panel.